Prediction of Individual Knee Kinematics From an MRI Representation of the Articular Surfaces

(Article begins on next page)

30 June 2024

Prediction of Individual Knee Kinematics from an MRI Representation of the Articular Surfaces

Michele Conconi, Nicola Sancisi and Vincenzo Parenti-Castelli

Abstract— *Objective*: **The knowledge of individual joint motion may help to understand the articular physiology and to design better treatments and medical devices. Measurements of in-vivo individual motion are nowadays invasive/ionizing (fluoroscopy) or imprecise (skin markers). We propose a new approach to derive the individual knee natural motion from a three-dimensional representation of articular surfaces.** *Methods*: **We hypothesize that tissue adaptation shapes articular surfaces to optimize load distribution. Thus, the knee natural motion is obtained as the envelope of tibiofemoral positions and orientations that minimize peak contact pressure, i.e. that maximize joint congruence. We investigated four in-vitro and one in-vivo knees. Articular surfaces were reconstructed from a reference MRI. Natural motion was computed by congruence maximization and results were validated versus experimental data, acquired through bone implanted markers, in-vitro, and single-plane fluoroscopy, in-vivo.** *Results*: **In two cases, one of which in-vivo, maximum mean absolute error stays below 2.2° and 2.7 mm for rotations and translations, respectively. The remaining knees showed differences in joint internal rotation between the reference MRI and experimental motion at 0° flexion, possibly due to some laxity. The same difference is found in the model predictions, which, however, still replicate the individual knee motion.** *Conclusion*: **The proposed approach allows the prediction of individual joint motion based on non-ionizing MRI data.** *Significance*: **This method may help to characterize healthy and, by comparison, pathological knee behavior. Moreover, it may provide an individual reference motion for the personalization of musculoskeletal models, opening the way to their clinical application.**

Index Terms— **Knee Natural Motion, Motion Prediction, Patient-specific Model, Joint Congruence, Functional Adaptation.**

I. INTRODUCTION

THE quantification of the individual joint motion, namely the relative displacements between the joint bones of a specific person, could help the identification of articular pathologies, the understanding of their etiology and the design of treatments and orthotic devices tailored on the patient needs [1-4]. This is particularly true for the tibiofemoral joint, one of the joints with the greatest mobility in the human body [5]. This articulation is also one of the most susceptible to ligament injuries and to the risk of osteoarthritis development [6].

The tibiofemoral motion, in absence of considerable external forces, is particularly significant. In these conditions, the abadduction (AA), internal-external rotation (IE) and the anteroposterior (AP), proximo-distal (PD) and medio-lateral (ML) translations are coupled to flexion-extension (FE). The unloaded tibiofemoral joint moves therefore on a one-DOF trajectory in the three-dimensional space, often referred to as passive or natural motion. A recent synthesis paper [7] showed that the

same coupling is substantially preserved during different physiological dynamic activities: external loads deform joint constraints and, consequently, modify the natural motion, whose characteristic pattern remains, however, still recognizable. The tibiofemoral joint may thus be thought as a compliant joint with a well-defined, one-DOF spatial trajectory, namely the knee natural motion. Moreover, experimental evidence showed that ligaments stay nearly isometric [8-10] and make no or the least work along this motion, also storing the least deformation energy [11]. Since the latter was associated with microdamage occurrence and accumulation [12], natural motion also minimizes the metabolic cost associated with tissue repairing and maintenance. These evidences suggest that the natural motion represents a mechanical optimum for the articulation.

An accurate estimation of joint motion is however difficult to obtain in-vivo. Non-invasive techniques that rely on skin-markers do not allow the precise description of the three-dimensional relative motion of the bones in a joint, mainly due to the soft tissue artefact [13,14]. Transcutaneous bone pins, although very accurate in slow dynamics, are invasive and can loosen, bend, and/or interfere with normal muscle action [15]. Biplanar video-radiographic systems enable a direct and accurate measurement of bone motion [16], but they expose the patient to ionizing radiation. MR scanners are limited to the investigation of quasi-static kinematics [17] and, in case of closed scanners, to a limited range of joint motion. More recently, MR scanners were also used for nearly real-time [18] or fully real-time [19] mono or multi-planar analysis of joint motion. This represents, however, a cutting-edge technology still to be developed. For all these reasons, the direct and accurate measure of the individual joint motion cannot be considered available for the current clinical practice.

Computational models can be used instead to predict quantities that cannot be measured directly in a clinical environment [20-22]. However, despite the great improvements in biomechanical modeling, prediction of joint kinematics is still challenging. Kinematic models evolved from simple revolute and spherical pairs to more complex planar [23] and spatial [24-29] parallel mechanisms, featuring a direct representation of the constraints imposed by ligaments and contacts. Similarly, multibody knee models with flexible elements evolved from planar [30] to spatial [31] systems, also featuring deformable contacts [32-34], several muscles [35] as well as a representation of the menisci [36, 37]. Finally, though normally devoted to static analyses at fixed flexion angles, finite element models were also used to investigate the moving knee [38-42]. All these

models highly contribute to explain the role of different anatomical structures in the guidance of joint motion and provide a good description of the average behavior of the knee. However, they generally need a preliminary tuning of their parameters [41-44] to become predictive for the single individual. This tuning is performed by minimizing the differences between model outcomes and some experimental data, typically a measurement of joint kinematics under known reference conditions [28,29,32,36,40].

A different approach to define a predictive model of the knee natural motion may rely on the identification of a physiological property that must be respected along the entire range of motion. Indeed, the energetic optimum of the natural motion described above is compatible with the capability of the joint tissues to modify their structure in response to the mechanical environment to which they are exposed [45-57]. This process, known as functional adaptation, is modulated by the loads and the motion in order to optimize the transmission of contact forces in the joint [58-61] and governs the development [62-64] and maintenance [65-70] of articular surfaces. We thus postulated that the final shape of articular surfaces is the result of an adaptation process, aiming at the optimization of the contact pressure distribution over the entire range of knee natural motion. This hypothesis relates the articular shape with its optimal working condition, similarly to what observed for the bone internal architecture [12,71-73], the ligament and tendon cross-section variations [74-75] and the morphogenesis of articulations [12,61,76,77]. Since the more congruent the articular surfaces, the smaller the peak contact pressure, the natural motion can thus be found by maximizing the joint congruence along the entire range of flexion. This concept was previously applied and validated for the tibiotalar joint [78].

The aim of this work is to verify whether the knee natural motion can be reconstructed from the shape of articular surfaces as the envelope of tibiofemoral positions and orientations that maximize the joint congruence. To this purpose, we investigated four in-vitro and one in-vivo knee. Model outcomes were validated using three different criteria: 1), directly, by comparing measured and predicted motions; 2), indirectly, by verifying whether the predicted motion is consistent with the joint anatomy, i.e. if it respects the ligament isometry; 3), indirectly, by comparing the predicted knee kinematics to the knee motion patterns of different physiological dynamic activities [7], to evaluate the physiological consistency of the model.

II. Materials and Methods

Note: All figures and table denoted with an *S* are in the supplementary material.

A. Clinical Images

Data measured on four lower-limb specimens and on a volunteer were considered. These data came from previous studies [11] and only main information is reported here.

Specimens were free from anatomical defects; the volunteer was healthy with no history of knee diseases. The donors and the participant information are reported in Table S1. For all legs, a detailed reference MRI of the knee was acquired for the

definition of the articular surfaces required by the kinematic model. Then, a detailed CT scan of the knee and a rougher CT scan of the whole leg were also acquired. Scanning parameters are reported in Table S2. Bones, articular surfaces, menisci and ligament insertions were then manually segmented from MRI using the free open-source software Medical Imaging Interaction Toolkit (MITK). Using the same software, detailed bone surfaces of the distal femur and proximal tibia and rougher surfaces of the whole leg were segmented from the CT scans by a thresholding criterion. MRI and CT data were registered based on bone surfaces through the ICP based registration tool of the commercial software Geomagic.

B. Anatomical Reference Systems and Motion Parametrization

Anatomical reference systems of the femur (S_f) and tibia (S_t) were defined on the CT-based bone surfaces of the whole leg by virtual palpation of anatomical landmarks according to a standardised convention [79]. Representation and definition of these reference systems are provided in Fig. S3.

Orientation of the tibia with respect to the femur was expressed according to a ZXY Euler angle sequence [80]: extension (+)/flexion(−), adduction (+)/abduction (−), internal (+)/external (−) rotations take place about the z, x and y axis of S_t respectively. The translations of the tibia with respect to the femur were represented as the coordinates of the S_t origin expressed in S_f, where anterior (+)/posterior (−), proximal (+)/distal (−), lateral (+)/medial (−) translations take place along the x, y and z axis of S_f respectively.

C. Measure of Joint Congruence

We developed a measure of joint congruence derived from the elastic foundation contact model [81]. With respect to the Hertzian contact model that holds only for non-conforming contacts [82-83], the elastic foundation contact model [84] is often employed when modelling joint contact [32,34,35,85-88]. In fact, the hypotheses behind elastic foundation model hold for both conforming and non-conforming contacts. In addition, elastic foundation represents a good approximation of the trabecular structure supporting the articular surfaces (Fig S2). For the sake of clarity and without loss of generality, the geometrical relation between applied load and peak pressure will be here derived for a simple nonconforming contact, as in Fig. 1.

Let us consider a rigid body indenting a mattress of springs of constant stiffness per unit area k (N/m³) resting on a rigid base, where no interaction between the adjacent springs is considered. Indentation force F is along axis z, while the plane perpendicular to z has axes x, y. If $\delta(x,y)$ is the deformation of the spring at position (x,y), the corresponding contact pressure can be expressed as

$$p(x, y) = k\delta(x, y) \qquad (1)$$

It follows that the peak pressure p_0 will take place at the position of maximum indentation $\varDelta$, namely

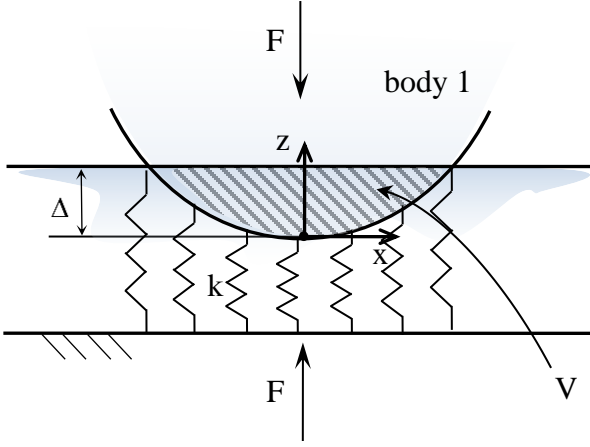$$p_0 = k\delta_{max} = k\Delta \qquad (2)$$

Figure 1: Schematization of the elastic foundation contact model.

If A is the projection of the contact surface on the plane xy, dA being the infinitesimal area on which a single spring acts, the resultant F of the pressure distribution is

$$F = \int_A p(x,y)dA = k\int_A \delta(x,y)dA = kV \tag{3}$$

where V is the volume of the Boolean intersection of the two undeformed bodies. This way, the ratio between the peak pressure and the resultant force becomes purely geometrical, i.e.

$$\frac{F}{p_0} = \frac{kV}{k\Delta} = \frac{V}{\Delta} \tag{4}$$

The ratio between intersection volume V and maximum indentation $\varDelta$ can thus be taken as a measure of joint congruence: the bigger this ratio, the higher the contact congruity, the lower the peak contact pressure. Once that a representation of the articular surfaces in a contact configuration is provided, it is thus possible to evaluate joint congruence by measuring the volume intersection between the undeformed surfaces and the maximum indentation. On the other hand, it is possible to use (4) in a numerical model, for instance by imposing the value of $\varDelta$ and searching for the joint configuration that maximizes V.

D. Computational Model

For every value of the flexion angle within the individual range of motion, approximately from 0° to 130°, the five coupled components of position and orientation of the tibia with respect to the femur were determined by an optimization algorithm.

The algorithm's objective function is a modification of (4), whose direct application would result in numerical instability. In fact, cartilage deformation tends to a plateau of about 5% of the original thickness, regardless of the performed activities [56]. Assuming a mean cartilage thickness of 2.5 mm for both the tibia and femur [89,90] will lead to a 0.25 mm of indentation. This value is below the usual in plane resolution of a MR scan, which can be estimated around 0.3 mm [90]. Using this
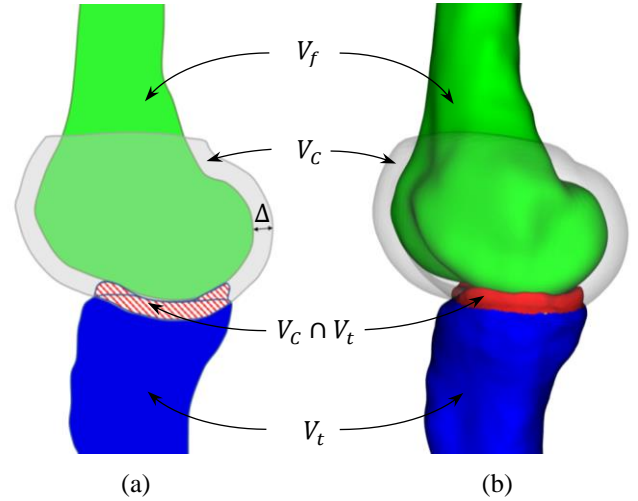

(a)   (b)

Figure 2: Cross sectional (a) and three-dimensional (b) representation of the elements contributing to the numerical evaluation of joint congruence.

value for $\varDelta$ would make the algorithm too sensitive to the quality of the MRI segmentation. To cope with this issue, one of the two contact surfaces was offset of a prescribed quantity $\varDelta$ and used in place of the original surface for congruence evaluation. This approach is similar to the proximity approximation often used for the evaluation of joint contact areas [83,91-93]. It was shown analytically that, for non-conforming contacts, this approach for congruence evaluation produces the same results of the relative curvature within the Hertz theory. In case of conforming contacts, an analogous theoretical comparison is not possible, but the application of this approach in other studies [78,94] showed that this measure is still representative of joint congruence. Finally, an additional term was added to penalize physically impossible configurations leading to co-penetration. Referring to Fig. 2, the objective function was thus:

$$f = V_C \cap V_t - k_p\left(V_t \cap V_f\right) \tag{5}$$

where V_f is the volume enclosed by the femur bone and cartilage together; V_t is the volume enclosed by the tibia bone and cartilage together, considering the menisci as part of the tibial plateau; V_C is the volume enclosed by an offset of $\varDelta$ of the V_f surface; k_p is a penalty scalar coefficient.

The parameter $\varDelta$ was chosen equal to 7 mm, higher than the mean meniscal peripheral thickness [95] in order to include their contribution in the congruence measure, while k_p was chosen equal to 20, a value that guarantees a residual co-penetration of the cartilage compatible with physiological values. However, a sensitivity analysis previously performed [96,97] showed that if k_p is above 10, the algorithm outcomes become almost insensitive to both k_p and $\varDelta$. Thus, these values were not further optimized nor changed among the subjects.

The algorithm was coded using C++: optimization relied on the Nelder-Mead Simplex algorithm as implemented in GSL (GNU Scientific Library), while Boolean operations needed for congruence evaluation were performed through GTS (GNU Triangulated Surface Library). The tibiofemoral configuration

measured on the reference MRI was taken as initial guess, setting the flexion value to zero. For any subsequent step, the initial guess was the configuration determined at the previous one, by imposing a 1° increment on the flexion angle. Sensitivity analysis showed that the optimization algorithm is robust with respect to the initial guess [97].

On a PC running Windows 10, with an Intel i7 processor (2.50 GHz) and 8 GB of RAM, the algorithm took about 30 minutes to compute one knee motion, in a range from 0° to 130° of flexion, with 1° steps. Results depended on the size of the STL representing the articular surfaces.

E. In-vitro evaluation of knee natural motion

Specimen motion measured in-vitro [11] was used for validation purposes. A surgeon removed the forefoot and all soft tissues except those at the joint, leaving the knee capsule and ligaments intact. A stereophotogrammetric system (Vicon Motion Systems Ltd) measured the tibia and femur relative motion by means of two trackers directly fixed to the bones. Each tracker included three markers. The specimen was mounted on a test rig for in-vitro analysis of the knee joint motion [98]: the femur was connected to the rig and was passively flexed while the tibia was free to move according to its natural motion (Fig. S1.a). Four screws were also inserted on each bone prior to the CT scans. The centre of the screw head was both manually segmented via MITK and digitized through the stereophotogrammetric system using a pointer. CT and stereophotogrammetric data were registered by least square fitting the centres of the screw heads. The tibiofemoral relative motion was then expressed in terms of relative motion between the corresponding anatomical reference systems. The accuracy of the whole in-vitro experimental setup was not quantified directly. However, considering the Vicon nominal accuracy and the tracker dimension, the accuracy in rigid body kinematics is reasonably below 1 mm for translations and 2° for rotations.

F. In-vivo evaluation of knee natural motion

Similarly, the in-vivo motion measured on the volunteer [99] was used to validate the model in-vivo. The present experiment was approved by the ethical committee at the Istituto Ortopedico Rizzoli, and the volunteer gave his informed consent. The natural motion of the participant was recorded by a single plane fluoroscopy (CAT Medical Systems, Hiris Rf43) as a series of sagittal images collected at 15 frame/s. The field of view was set to record the knee, half tibia and half femur. The experiment was designed to minimize the muscle activation in the volunteer's leg. The volunteer was asked to perform a full flexion-extension movement starting with the leg fully extended. The task was performed with the volunteer half-lying on a smooth plane, by pulling the leg towards the chest up to full flexion with the aid of a lace tied around the thigh (Fig. S1.b), and then by letting the leg extend back to full extension. The heel of the subject was placed on a polytetrafluoroethylene disk to reduce friction with the plane. The CT-based bone surfaces of the femur and tibia were manually registered on the fluoroscopy images using a dedicated software [100]. Again, the tibiofemoral relative motion was then expressed in terms of

relative motion between the corresponding anatomical reference systems. The theoretical accuracy in tibio-femoral motion reconstruction by means of monoplanar fluoroscopy can be estimated in 2 mm for sagittal plane displacements, 7.5mm for medial/lateral displacement, and 1.5 deg for all rotations [101].

G. Evaluation of ligament isometry

For each ligament, the most isometric fiber was identified as the line connecting two points (one on the tibial, the other on the femoral insertion areas) that showed the smallest maximum percent length variation, during both the predicted and measured motions, as done in [25,28,29,44]. The maximum percent length variation in each ligament fiber was computed as:

$$\%\Delta L = \frac{L_{max} - L_{min}}{L_{max}} \cdot 100 \qquad (6)$$

and values minor or equal to five percent were considered representative of isometry [12]. This limit denotes the end of the toe region of the ligament stress-strain curve, corresponding to the fiber un-crimping.

III. RESULTS

Model predictions and experimental measures were compared through the mean absolute error (MAE), computed for each of the coupled motion components over the individual range of flexion. Table 1 shows the MAE for each subject and component. Errors on the AA are below 1.5°, while the IE shows more variability with a maximum error of 9.1°. For the first two legs, whose IE error is below 2.2°, translational errors remain below 3.4 mm. Where the IE error is higher, translational errors (in particular AP and PD) are also higher, though below 8 mm.

Predicted and measured motion patterns were qualitatively compared in terms of motion components in Fig. 3 and in terms of instantaneous helical axis (IHA) envelope in Fig. S4, the latter computed according to [102]. The tibial internal rotation pattern is correctly predicted by the model, though in three knees predictions and measurements differ by an almost constant quantity. The same difference was however observed between experimental motion at 0° flexion and the knee configuration measured on the reference MRI (Fig. 3): this latter (black dots) is closer to the model predictions (red curves) than to the experimental motion (blue curves). In Fig 4, both predicted and measured motions are represented with tibiofemoral motions

Table 1:Mean absolute error (MAE) between predicted and experimental motion components. In-vivo leg is denoted with a star.

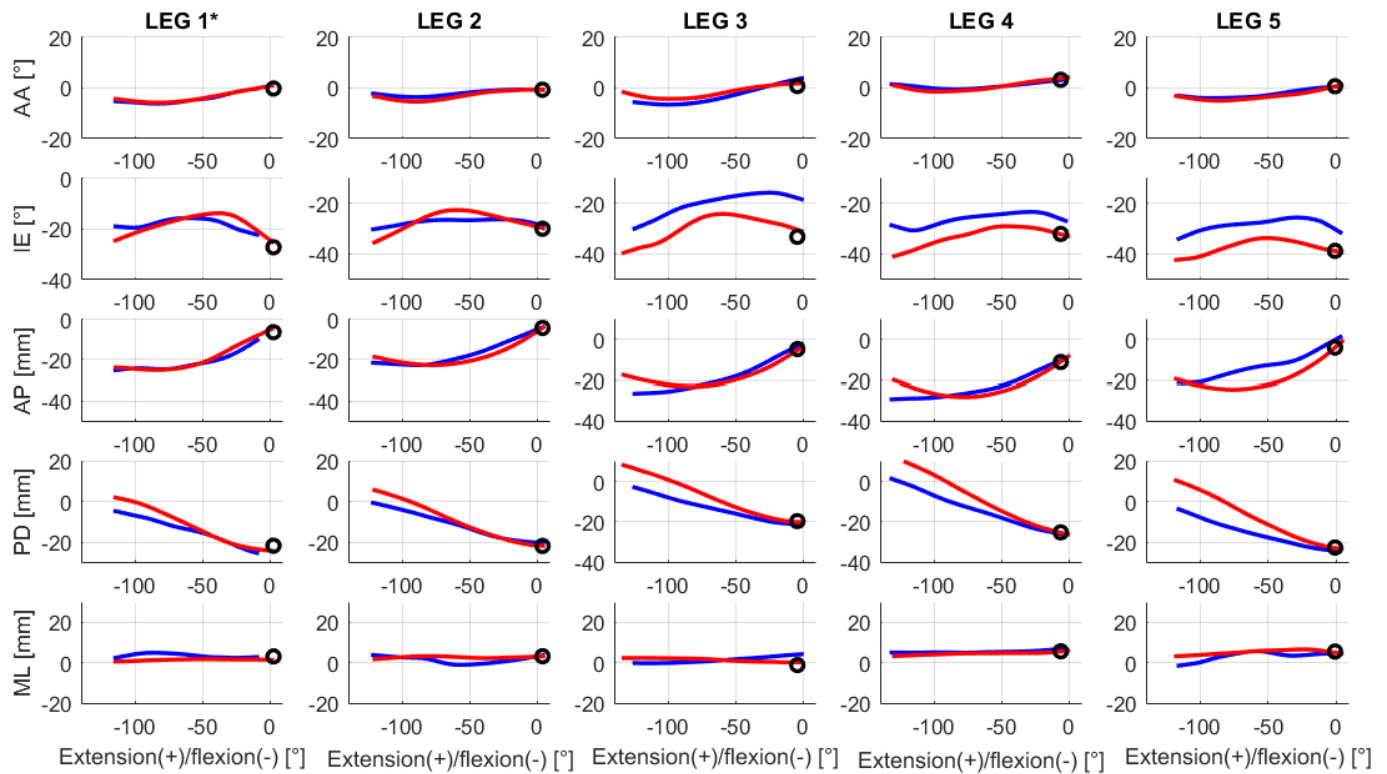|	Leg 1*	Leg 2	Leg 3	Leg 4	Leg 5
AA [°]	1.2±0.5	1.0±0.6	1.7±0.7	0.7±0.4	0.8±0.3
IE [°]	2.2±1.9	2.2±1.4	9.1±2.2	6.7±1.5	8.7±1.4
AP [°]	1.3±0.5	2.0±1.1	2.5±1.5	2.8±1.7	6.0±3.0
PD [mm]	3.4±3.1	2.6±2.2	5.0±3.3	5.8±4.0	7.5±4.6
ML [mm]	2.7±1.1	1.8±1.2	1.8±0.9	1.0±0.4	1.9±1.4

Figure 3: Comparison between predicted (red) and measured (blue) motion on the abb-abduction angle (AA), internal-external rotation (IE), antero-posterior (AP), proximo-distal (PD) and medio-lateral (ML) translations for each knee. In-vivo leg is denoted with a star. Black dots represent the knee configuration measured on reference MRI.
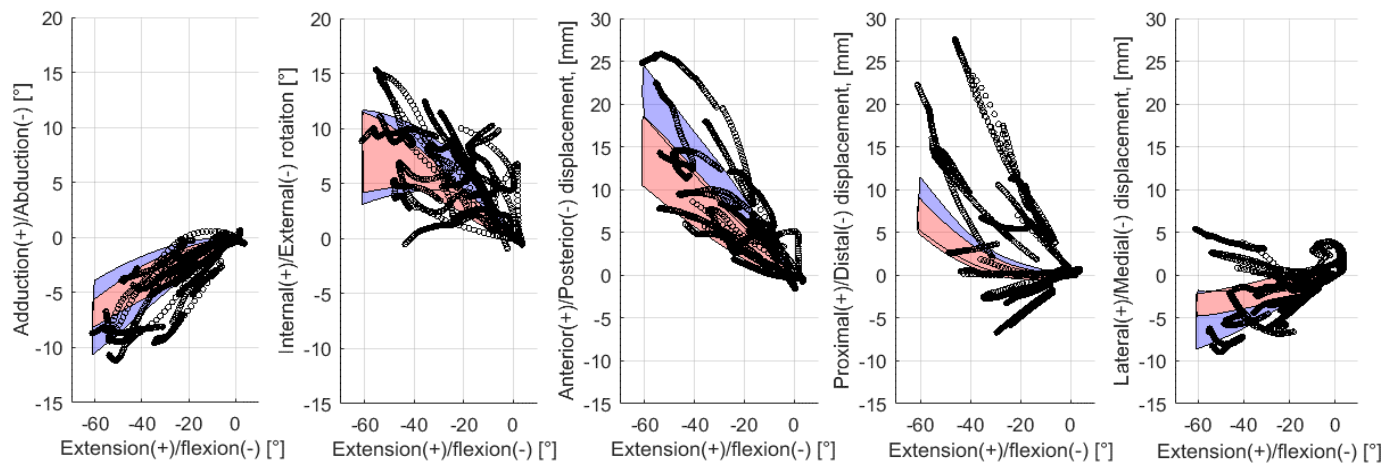

Figure 4: Representation of the envelope of predicted (red) and measured (blue) knee motion for the five analyzed knees with respect to the knee motion under different dynamic tasks (black dots), namely, walking, drop landing, hopping, stair-ascending, running, and cutting [7].

Table 2:Maximum percent elongation of anterior cruciate (ACL), posterior cruciate (PCL), medial (MCL) and lateral (LCL) collateral ligament for predicted (Pred) and measured (Meas) motion for each knee. Red and blue numbers represent a maximum elongation greater than 5% for the predicted and measured results respectively. In-vivo leg is denoted with a star.

	ACL		PCL		MCL		LCL	
	Pred	**Meas**	**Pred**	**Meas**	**Pred**	**Meas**	**Pred**	**Meas**
Leg 1*	7.1	13.0	18.9	9.2	0.1	2.6	14.8	14.5
Leg 2	4.1	2.1	3.8	1.6	2.8	3.0	2.1	1.6
Leg 3	3.6	3.5	9.9	5.1	1.8	3.2	2.0	1.7
Leg 4	3.1	2.5	11.1	2.6	1.6	1.2	1.1	1.9
Leg 5	14.0	7.1	5.0	3.2	1.7	1.8	1.5	1.9

during different dynamic activities [7]. For the sake of this comparison, the tibia reference system of each subject was chosen so that, at 0° flexion all the other DOF are also set to zero, following the approach proposed in [7]. Both predicted and measured motions fall well within the tibiofemoral trajectories in dynamic conditions.

The model was evaluated also in terms of deformation energy, by comparing the obtained ligament isometry to that observed with experimental motion. Table 2 reports the results of Eq. (6) for each ligament and subject. Over the 20 considered ligaments, only 4 show a less isometric behavior during experiments, and 3 of them are related to the in-vivo leg. The model correctly predicts the higher or lower isometric behavior, except for the PCL of legs 4.

IV. Discussion

The aim to this work was to present and validate a kinematic model that predicts individual knee natural motion based on the shape of articular surfaces, here derived from MRI.

The model performance was evaluated directly, by comparing model outcomes with experimental data for each subject. From a qualitative point of view, the model predictions describe well both the coupling between the internal rotation and flexion, and the typical IHA pattern of the knee natural motion (Fig. 3 and S4). From a quantitative point of view, the agreement between model predictions and experimental measures is better of or comparable with other patient-specific knee models [28,29,32,36,37,40,42]. It is worth noting that the accuracy of those models was reached after tuning the model parameters to fit some preliminary kinematic data. On the contrary, the congruence model is fully predictive. The differences in accuracy of the congruence models is related to the reference MRI. When the tibiofemoral configuration observable in reference MRI (black dots in Fig. 3) is close to the experimental motion at 0° flexion (legs 1 and 2), the MAE stays below 2.2° for the rotations and 3.4 mm for the translations. On the contrary, when the reference MRI configuration is far from the experimental motion at 0° flexion (legs 3, 4, and 5), the MAEs increase. The difference between the reference MRI configuration and experimental motion at 0° flexion can be due to a higher knee laxity in connection with other experimental uncertainties, mainly affecting the IE rotation. The same initial difference also affects the model outcome, resulting in an almost constant error on the IE rotation (maximum standard deviation of the difference is 2.2°). This can be explained by considering that the congruence model is guided also by the menisci, whose position on the tibial plateau is rigidly defined by the reference MRI. Since menisci contribute to the joint congruence, a variation in their position will be reflected in the prediction of the congruence model, which in fact always passes through the configuration of the refence MR scan. This could explain the observed offset in the intra/extra rotation in the predicted motion. Also, these rotational differences partially explain the discrepancies on translational motion components on the last three legs: the tibia is more externally rotated during experimental motion, inducing a proximal displacement of the lateral plateau as well as of the S_t origin at higher flexion angles (Fig. S5). As a result, an

external rotation is coupled with a posterior translation, in agreement with the results of Table 1 and Fig 3. The lower accuracy observed in leg 3, 4, and 5 are therefore ascribable mainly to differences between reference MRI and experimental motion.

The model performance was also indirectly assessed by evaluating the ligament isometry for each subject and comparing model outcomes with average experimental dynamic data. The predicted motions fall well within the range of knee motions associated with typical dynamic activities (Fig. 4) [7]. This result confirms the physiological consistency of the model and provides an indirect confirmation of the main hypothesis beyond it: the natural knee motion represents a mechanical optimum from which loaded motions derive when ligament deformations take place. This is confirmed also in terms of ligament elongation: the model could correctly predict the isometric behavior of 19 out of 20 total ligaments, thus resulting also consistent with the joint anatomy.

The presented approach may provide insights in the articular physiology, allowing the characterization of healthy behavior and, by comparison, the identification of articular pathology, possibly helping to understand their etiology. Moreover, with respect to other techniques for the modeling of the knee motion, the proposed approach has several advantages: it is accurate with respect to the current literature, it does not require invasive/ionizing exams, and it can be integrated easily within the clinical practice, requiring only MRI of the joint. Finally, the proposed approach is general and thus extendable to other articulations, as shown for the tibiotalar joint [78]. The knowledge of individual knee motion can be used to optimize placement of commercial prostheses, by improving the knee balancing [103] or refining a kinematic alignment [104]. Moreover, since the predicted motion respects ligament isometry, it can be used in combination with 3D printing technology to design naturally-balanced personalized prostheses [105].

The kinematic model here presented can also be used for the personalization of musculoskeletal models, a theme recognized as a key point for their future development [106-108]. The model outcomes could be directly used to prescribe the patient-specific tibiofemoral kinematics, similarly to what done with average in-vitro motions [109] within the OpenSim model proposed by Rajagopal et al. [110]. Also, the combination of individual kinematics and articular surfaces makes it possible to identify patient-specific pattern of contact points and normals, possibly improving the computation of joint contact forces through musculoskeletal models. Furthermore, a measure of joint congruence could be used directly within a cost function for the inverse kinematics computation in motion analysis. Alternatively, the predicted motion can be used as a reference for the synthesis of personalized knee kinematic models, starting from simple hinges or spherical pairs, for which optimal revolute axes and rotation centers can be defined, up to parallel mechanisms featuring the contribution of ligaments and contacts [14,111,111]. Finally, the model predictions can be used for the tuning of ligament and contact parameters in multibody or FEM models [32,36,52]. In particular, a recent study [113]

showed that a standard knee planar simplification [114] generated ligament elongations up to 56%. Excessive ligament elongation reduces the reliability of musculoskeletal model outcomes, particularly when joint reaction analysis is performed: on one hand, it denotes a non-physiological knee motion; on the other hand, it makes the contribution of ligaments to joint equilibrium no longer negligible, a hypothesis often employed within musculoskeletal models. The approach here presented may offer a possible way to overcome this problem, providing joint models that are anatomically consistent. Finally, the possibility to define accurate and patient-specific joint models may improve the performance of multibody optimization techniques, reducing the impact of soft-tissue artefacts on kinematics estimation from skin marker motion [107, 115-118].

This work has limitations. Menisci are modelled as a rigid extension of the tibial cartilage. This oversimplification is dictated by the reported low meniscal mobility [119] and by the necessity to include the menisci in the model while keeping an acceptable computational burden [120], but it makes the scanning configuration of the reference MRI crucial. Nevertheless, the impact of this hypothesis remains to be determined: when reference MRI configuration belongs to the measured motion, model predictions show a remarkable agreement despite the rigid menisci. A wider investigation on this topic would be however beneficial.

The number of legs is not high to claim a solid validation. In particular, more in-vivo knees need to be investigated. Also, the comparison of model outcome with dynamic activities is based on aggregate motion patterns from different studies [7]. The employed average dynamic data may thus suffer from the uncertainties typical of synthesis analysis paper. Individual dynamic data should be collected to evaluate the relation between natural motion and dynamic tasks for the single subject. In this direction, we are currently undergoing an experimental campaign investigating knee kinematics through dynamic MRI in an orthostatic open scanner. Preliminary data from three knees support the result of the present analysis.

The model relies on the quality of the articular surfaces' reconstruction. Accurate cartilage segmentation is generally a manual procedure. Although preliminary investigation has shown that model outcomes are quite robust to variation in cartilage segmentation, a systematic analysis of the model sensitivity to inter- and intra-operator reconstruction of cartilage is still needed. Similarly, derivation of the model from more readily available and cost-effective CT scans deserve to be investigated.

Finally, the model main assumption is that articular shape is the result of tissue adaptation to loads. This is relevant for healthy tissues, but the direct application to a pathological population must be considered carefully. In case of traumatic injuries, the presented model holds as long as the time between injury and the analysis does not allow a considerable remodeling of the knee structures. On the other side, its application to severe and congenital deformities may result incorrect. Further investigations would however be deserved.

V. CONCLUSION

In this paper, a new model able to predict the three-dimensional motion of individual knees has been presented and validated. It relies on a three-dimensional representation of the articular surfaces, which can be obtained from standard MRI. Thus, it may represent a clinically valuable alternative to the current methods for measuring the knee motion. The outcomes of the model provide useful information about knee physiology per se. In addition, a quantification of the individual joint motion can be used as a reference for the definition of more advanced, patient-specific musculoskeletal models, opening the way to their clinical application.

ACKNOWLEDGMENT

REFERENCES

[1] J. R. Davids et al., "Optimization of walking ability of children with cerebral palsy," *JBJS*, vol. 85, no.11, pp.2224-2234, 2003

[2] R. A. Malinzak et al., "A comparison of knee joint motion patterns between men and women in selected athletic tasks," *Clin Biomech (Bristol, Avon)*, vol. 16, no.5, pp.438-445, 2001.

[3] M. S. Coats-Thomas et al., "Effects of ACL reconstruction surgery on muscle activity of the lower limb during a jump-cut maneuver in males and females," *J. Orthop. Res*., vol. 31, no.12, pp.1890-1896, 2013.

[4] H. Kurosawa et al., "Load-bearing mode of the knee joint: physical behavior of the knee joint with or without menisci," *Clin. Orthop. Relat. Res.,* no.149, pp.283-290, 1980.

[5] A. M. J. Bull and A. A. Amis, "Knee joint motion: Description and measurement," *Proc Inst Mech Eng H*, vol. 212, no.5, pp.357-372, 1998.

[6] D. Prieto-Alhambra et al., "Incidence and risk factors for clinically diagnosed knee, hip and hand osteoarthritis: influences of age, gender and osteoarthritis affecting other joints," *Ann. Rheum. Dis.,* vol. 73, no.9, pp.1659-1664, 2014.

[7] X. Gasparutto et al., "Kinematics of the Normal Knee during Dynamic Activities: A Synthesis of Data from Intracortical Pins and Biplane Imaging," *Appl Bionics Biomech*, vol. 2017, pp.1908618, 2017.

[8] D. Wilson et al., "The components of passive knee movement are coupled to flexion angle," *J Biomech*, vol. 33, no.4, pp.465-473, 2000.

[9] C. Belvedere et al., "Geometrical changes of knee ligaments and patellar tendon during passive flexion," *J Biomech*, vol. 45, no.11, pp.1886-1892, 2012.

[10] J. Victor et al., "How isometric are the medial patellofemoral, superficial medial collateral, and lateral collateral ligaments of the knee?," *Am J Sports Med*, vol. 37, no.10, pp.2028-2036, 2009.

[11] M. Conconi et al., "The Geometrical Arrangement of Knee Constraints that Makes Natural Motion Possible: Theoretical and Experimental Analysis," *J Biomech Eng,* vol. 141, no. 5, pp. 051001-6, 2019.

[12] D. R. Carter, "Mechanical loading history and skeletal biology," *J Biomech*, vol. 20, pp.1095-1109, 1987.

[13] V. Camomilla, R. Dumas and A. Cappozzo "Human movement analysis: The soft tissue artefact issue". *J Biomech*, vol 62, pp. 1-4, 2017.

[14] A. Leardini et al., "Kinematic models of lower limb joints for musculoskeletal modelling and optimization in gait analysis," *J Biomech*, vol. 62, pp.77-86, 2017.

[15] D. K. Ramsey et al., "Methodological concerns using intra-cortical pins to measure tibiofemoral kinematics," *Knee Surg Sports Traumatol Arthrosc*, vol. 11, no.5, pp.344-349, 2003.

[16] D. L. Miranda et al., "Static and dynamic error of a biplanar videoradiography system using marker-based and markerless tracking techniques," *J Biomech Eng,* vol. 133, no.12, pp.121002, 2011.

[17] V. V. Patel et al., "A three-dimensional MRI analysis of knee kinematics," J. Orthop. Res., vol. 22, no.2, pp.283-292, 2004.

[18] F. T. Sheehan et al., "Using cine phase contrast magnetic resonance imaging to non-invasively study in vivo knee dynamics," *J Biomech*, vol. 31, no.1, pp.21-26, 1998.

[19] R. D. Boutin et al., "Real-time magnetic resonance imaging (MRI) during active wrist motion--initial observations," PLoS ONE, vol. 8, no.12, pp. e84004, 2013.

[20] M. G. Pandy, "Computer modeling and simulation of human movement," *Ann Rev Biomed Eng,* vol. 3, no.1, pp.245-273, 2001.

[21] A. Erdemir et al., "Model-based estimation of muscle forces exerted during movements," *Clin Biomech,* vol. 22, no.2, pp.131-154, 2007.

[22] B. J. Fregly et al., "Grand challenge competition to predict in vivo knee loads," J Orth Res, vol. 30, no.4, pp.503-513, 2012.

[23] H. Straßer. (1917). Lehrbuch der Muskel-und Gelenkmechanik: Die untere Extremitaet. Springer.

[24] D. R. Wilson et al., "Ligaments and articular contact guide passive knee flexion," *J Biomech*, vol. 31, no.12, pp.1127-1136, 1998.

[25] R. Di Gregorio and V. Parenti-Castelli, "A spatial mechanism with higher pairs for modelling the human knee joint," *J Biomech Eng*, vol. 125, no.2, pp.232-237, 2003.

[26] J. Feikes et al., "A constraint-based approach to modelling the mobility of the human knee joint," *J Biomech*, vol. 36, no.1, pp.125-129, 2003.

[27] A. Ottoboni et al., "Articular surface approximation in equivalent spatial parallel mechanism models of the human knee joint," *Proc Inst Mech Eng H*, vol. 224, no.9, pp.1121-1132, 2010.

[28] N. Sancisi and V. Parenti-Castelli, "A 1-dof parallel spherical wrist for the modelling of the knee passive motion," Mech Mach Theory, vol. 45, no.4, pp.658-665, 2010.

[29] N. Sancisi and V. Parenti-Castelli, "A novel 3d parallel mechanism for the passive motion simulation of the patella-femur-tibia complex," *Meccanica*, vol. 46, no.1, pp.207-220, 2011.

[30] H. Gill and J. O'Connor, "Biarticulating two-dimensional computer model of the human patellofemoral joint," *Clin Biomech*, vol. 11, no.2, pp.81-89, 1996.

[31] J. Wismans et al., "A three-dimensional mathematical model of the knee-joint," *J Biomech*, vol. 13, no.8, pp.677-685,1 980.

[32] L. Blankevoort and R. Huiskes, "Validation of a three-dimensional model of the knee," *J Biomech*, vol. 29, no.7, pp.955-961, 1996.

[33] I. Sintini et al., "Comparison between anatomical and approximate surfaces in a 3D kinetostatic model of the knee for the study of the unloaded and loaded joint motion," *Meccanica*, vol. 53, no.1, pp.7-20, 2018.

[34] D. I. Caruntu and M. S. Hefzy, "3-D anatomically based dynamic modeling of the human knee to include tibio-femoral and patello-femoral joints," *J Biomeh Eng*, vol. 126, no.1, pp.44-53, 2004.

[35] M. G. Pandy et al., "A three-dimensional musculoskeletal model of the human knee joint. Part 1: theoretical construction," *Comput Method Biomec*, vol. 1, no.2, pp.87-108, .1997.

[36] T. M. Guess et al., "A subject specific multibody model of the knee with menisci," *Med Eng&Phy*, vol. 32, no.5, pp.505-515, 2010.

[37] M. Kia et al., "A multibody knee model corroborates subject-specific experimental measurements of low ligament forces and kinematic coupling during passive flexion". *J Biomech Eng*, vol. 138, no. 5, pp. 051010_1-12, 2016.

[38] G. Li et al., "A validated three-dimensional computational model of a human knee joint," *J Biomech Eng*, vol. 121, no.6, pp.657-662, 1999.

[39] M. Adouni et al., "Computational biodynamics of human knee joint in gait: from muscle forces to cartilage stresses," *J Biomech*, vol. 45, no.12, pp.2149-2156, 2012.

[40] R. Mootanah et al., "Development and validation of a computational model of the knee joint for the evaluation of surgical treatments for osteoarthritis," *Comput Method Biomec*, vol. 17, no.13, pp.1502-1517, 2014.

[41] P. Beillas et al., "A new method to investigate in vivo knee behavior using a finite element model of the lower limb," *J Biomech*, vol. 37, no.7, pp.1019-1030, 2004

[42] M. D. Harris et al., "A combined experimental and computational approach to subject-specific analysis of knee joint laxity" *J of Biomech Eng*, vol. 138, no. 8, pp. 081004_1-8, 2016.

[43] Y. Jung et al., "Intra-articular knee contact force estimation during walking using force-reaction elements and subject-specific joint model," J Biomech Eng, vol. 138, no.2, pp.021016, 2016.

[44] N. Sancisi and V. Parenti-Castelli, "A sequentially-defined stiffness model of the knee," *Mech Mach Theory*, vol. 46, no.12, pp.1920-1928, 2011.

[45] H. M. Frost, "Skeletal structural adaptations to mechanical usage (SATMU): 1-4," *Anat. Rec.,* vol. 226, pp.403-439, 1990.

[46] S. Judex et al., "Strain gradients correlate with sites of exercise-induced bone-forming surfaces in the adult skeleton," *J. Bone Miner. Res.*, vol. 12, pp.1737-1745, 1997.

[47] Y. F. Hsieh and C. H. Turner, "Effects of loading frequency on mechanically induced bone formation," *J. Bone Miner. Res.,* vol. 16, pp.918-924, 2001.

[48] J. L. Schriefer et al., "Cellular accommodation and the response of bone to mechanical loading," *J Biomech*, vol. 38, pp.1838-1845, 2005.

[49] C. M. Tipton et al., "Experimental studies on the influences of physical activity on ligaments, tendons and joints: a brief review," *Acta Med. Scand. Suppl.,* vol. 711, pp.157-168, 1986.

[50] K. Hayashi, "Biomechanical studies of the remodeling of knee joint tendons and ligaments," *J Biomech*, vol. 29, no.6, pp.707-716, 1996.

[51] H. Fujie et al., "Effects of growth on the response of the rabbit patellar tendon to stress shielding: a biomechanical study," *Clin Biomech (Bristol, Avon)*, vol. 15, pp.370-378, 2000.

[52] M. Benjamin and J. R. Ralphs, "Fibrocartilage in tendons and ligaments-an adaptation to compressive load," *J. Anat.*, vol. 193, no. 4, pp.481-494, 1998.

[53] H. J. J. Blackwood, "Cellular remodeling in articular tissue," *J Dent Res*, vol. 43, no.3, pp.480-489, 1966.

[54] M. Hudelmaier et al., "Correlation of knee-joint cartilage morphology with muscle cross-sectional areas vs. anthropometric variables," *Anat Rec A Discov Mol Cell Evol Biol*, vol. 270, pp.175-184, 2003.

[55] F. Eckstein et al., "The effects of exercise on human articular cartilage," *J. Anat.*, vol. 208, pp.491-512, 2006.

[56] H. Brommer et al., "Functional adaptation of articular cartilage from birth to maturity under the influence of loading: a biomechanical analysis," *Equine Vet. J.*, vol. 37, pp.148-154, 2005.

[57] J. H. Plochocki et al., "Functional adaptation of the femoral head to voluntary exercise," *Anat Rec A Discov Mol Cell Evol Biol*, vol. 288, pp.776-781, 2006.

[58] E. L. Radin et al., "Effect of repetitive impulsive loading on the knee joints of rabbits," *Clin. Orthop. Relat. Res.*, no.131, pp.288-293, 1978.

[59] P. G. Bullough, "The geometry of diarthrodial joints, its physiologic maintenance, and the possible significance of age-related changes in geometry-to-load distribution and the development of osteoarthritis," *Clin. Orthop. Relat. Res.,* vol. 156, no.156, pp.61-66, 1981.

[60] H. M. Frost, "An approach to estimating bone and joint loads and muscle strength in living subjects and skeletal remains," *Am. J. Hum. Biol.*, vol. 11, pp.437-455, 1999.

[61] J. H. Heegaard et al., "Mechanically modulated cartilage growth may regulate joint surface morphogenesis," *J. Orthop. Res.*, vol. 17, pp.509-517, 1999.

[62] J. H. McMaster and C. R. Weinert, "Effects of mechanical forces on growing cartilage," *Clin. Orthop. Relat. Res.*, vol. 72, pp.308-314, 1970.

[63] D. Ruano-Gil et al., "Embryonal hypermobility and articular development," *Acta Anat (Basel)*, vol. 123, pp.90-92, 1985.

[64] A. C. Ward and A. Pitsillidcs, "Developmental immobilization induces failure of joint cavity formation by a process involving selective local changes in glycosaminoglycan synthesis," *Trans Orthop Res Soc*, vol. 40, pp.199, 1998.

[65] M. J. Palmoski et al., "Joint motion in the absence of normal loading does not maintain normal articular cartilage," *Arthritis Rheum.*, vol. 23, pp.325-334, 1980.

[66] K. Paukkonen et al., "Quantitative morphological and biochemical investigations on the effects of physical exercise and immobilization on the articular cartilage of young rabbits," *Acta. Biol. Hung.*, vol. 35, pp.293-304, 1984.

[67] M. Bouvier and M. L. Zimny, "Effects of mechanical loading on surface morphology of the condylar cartilage of the mandible in rats," *Acta Anat (Basel),* vol. 129, pp.293–300, 1987.

[68] K. M. O'Connor, "Unweighting accelerates tidemark advancement in articular cartilage at the knee joint of rats," *J. Bone Miner. Res.*, vol. 12, pp.580-589, 1997.

[69] B. Vanwanseele et al., "Knee cartilage of spinal cord-injured patients displays progressive thinning in the absence of normal joint loading and movement," *Arthritis Rheum.*, vol. 46, pp.2073-2078, 2002.

[70] T. P. Andriacchi et al., "Gait mechanics influence healthy cartilage morphology and osteoarthritis of the knee," *J Bone Joint Surg Am*, vol. 91 Suppl 1, pp.95-101, 2009.

[71] R. Huiskes et al., "Adaptive bone-remodeling theory applied to prosthetic-design analysis," *J Biomech*, vol. 20, pp.1135-1150, 1987.

[72] I. G. Jang and I. Y. Kim, "Computational study of Wolff's law with trabecular architecture in the human proximal femur using topology optimization," *J Biomech*, vol. 41, pp.2353-2361, 2008.

[73] A. Vahdati and G. Rouhi, "A model for mechanical adaptation of trabecular bone incorporating cellular accommodation and effects of microdamage and disuse," *Mech. Res. Commun.*, vol. 36, no.3, pp.284-293, 2009.

[74] N. J. Giori et al., "Cellular shape and pressure may mediate mechanical control of tissue composition in tendons," *J. Orthop. Res.,* vol. 11, pp.581-591, 1993.

[75] T. A. Wren et al., "Tendon and ligament adaptation to exercise, immobilization, and remobilization," *J Rehabil Res Dev*, vol. 37, no.2, pp.217-224, 2000.

[76] D. R. Carter and M. Wong, "The role of mechanical loading histories in the development of diarthrodial joints," *J. Orthop. Res.*, vol. 6, pp.804-816, 1988.

[77] D. R. Carter et al., "The mechanobiology of articular cartilage development and degeneration," *Clin. Orthop. Relat. Res.,* vol. 427 S, pp.69-77, 2004.

[78] M. Conconi et al., "Joint kinematics from functional adaptation: A validation on the tibio-talar articulation," *J Biomech*, vol. 48, no.12, pp.2960-2967, 2015.

[79] G. Wu and P. R. Cavanagh, "ISB recommendations for standardization in the reporting of kinematic data," *J Biomech*, vol. 28, no.10, pp.1257-1261, 1995.

[80] E. S. Grood and W. J. Suntay, "A Joint Coordinate Systenf for the Clinical Description of Three-Dimensional Motions: Application to the Knee," *J Biomech Eng*, vol. 135, pp.136-144, 1983.

[81] M. Conconi and V. Parenti-Castelli, "A sound and efficient measure of joint congruence," *Proc. of IMechE Part* H, vol. 228, no.9, pp.935-941, 2014.

[82] G. Ateshian et al., "Curvature characteristics and congruence of the thumb carpometacarpal joint: differences between female and male joints," *J Biomech*, vol. 25, no.6, pp.591-607, 1992.

[83] K. Connolly et al., "Analysis techniques for congruence of the patellofemoral joint," *J Biomech Eng*, vol. 131, no. 12, pp.124503-1-7, 2009.

[84] K. Johnson. (1985), Contact mechanics. Cambridge: Cambridge University Press.

[85] Y. Bei and B. J. Fregly, "Multibody dynamic simulation of knee contact mechanics," *Med Eng& Phy*, vol. 26, no.9, pp.777-789, 2004.

[86] D. D. Anderson et al., "Implementation of discrete element analysis for subject-specific, population-wide investigations of habitual contact stress exposure," *J Appl Biomech*, vol. 26, no.2, pp.215-223, 2010.

[87] C. L. Abraham et al., "A new discrete element analysis method for predicting hip joint contact stresses," *J Biomech*, vol. 46, no.6, pp.1121-1127, 2013.

[88] A. M. Kern and D. D. Anderson, "Expedited patient-specific assessment of contact stress exposure in the ankle joint following definitive articular fracture reduction," *J Biomech*, vol. 48, no.12, pp.3427-3432, 2015.

[89] D.E. Shepherd and B.B. Seedhom, "Thickness of human articular cartilage in joints of the lower limb," *Ann. Rheum. Dis.*, vol. 58, pp.27-34, 1999.

[90] M. E. Bowers et al., "Quantitative MR imaging using "LiveWire" to measure tibiofemoral articular cartilage thickness," *Osteoarthr. Cartil.*, vol. 16, no.10, pp.1167-1173, 2008.

[91] G. A. Ateshian et al., "A stereophotogrammetric method for determining in situ contact areas in diarthrodial joints, and a comparison with other methods," *J Biomech,* vol. 27, no.1, pp.111-124, 1994.

[92] W.J. Anderst and S. Tashman, "A method to estimate in vivo dynamic articular surface interaction," *J Biomech*, vol.36, no.9, pp.1291-99, 2003.

[93] F. Corazza et al., "Articular contact at the tibiotalar joint in passive flexion," *J Biomech*, vol. 38, no.6, pp.1205-1212, 2005.

[94] M. Conconi et al., "Is early osteoarthritis associated with differences in joint congruence?," *J Biomech*, vol. 47, no.16, pp.3787-3793, 2014.

[95] P. Braz and W. Silva, "Meniscus morphometric study in humans," *J. Morphol. Sci.*, vol. 27, no.2, pp.62-66, 2010.

[96] M. Conconi and V. Parenti Castelli, "Joint kinematics from functional adaptation: an application to the human ankle," *AMM*, vol. 162, pp.266-275, 2012.

[97] M. Conconi and V. Parenti-Castelli, "Sensitivity and Stability Analysis of a Kinematic Model for Human Joints (An Application to Human Ankle)," In: *XII International Symposium on 3D Analysis of Human Movement*, 2012, pp.1-4.

[98] M. Forlani et al., "A new test rig for static and dynamic evaluation of knee motion based on a cable-driven parallel manipulator loading system," *Meccanica*, vol. 51, no.7, pp.1571-1581, 2016.

[99] F. Nardini et al., "An Anatomical-Based Subject-Specific Model of In-Vivo Knee Joint 3D Kinematics From Medical Imaging," Applied Sciences, vol. 10, no. 6, pp. 2100-2113, 2020.

[100] S. A. Banks and W. A. Hodge, "Accurate measurement of three-dimensional knee replacement kinematics using single-plane fluoroscopy," *IEEE Trans Biomed Eng*, vol. 43, no.6, pp.638-649, 1996.

[101] B.J. Fregly, H.A. Rahman and S.A. Banks, "Theoretical accuracy of model-based shape matching for measuring natural knee kinematics with single-plane fluoroscopy", J Biomec Eng, vol.127, no. 4, pp.692-9, 2005.

[102] L. W. Tsai. (1999), Robot analysis: the mechanics of serial and parallel manipulators. John Wiley & Sons.

[103] M. C. Meloni et al., "Soft tissue balancing in total knee arthroplasty," *Joints*, vol. 2, no.1, pp.37, 2014.

[104] S. M. Howell et al., "Does a kinematically aligned total knee arthroplasty restore function without failure regardless of alignment category?," *Clin. Orthop. Relat. Res.,* vol. 471, no.3, pp.1000-1007, 2013.

[105] E. Liverani et al., "Fabrication Of Knee Prostheses By Means Of SLM: Process And Functional Characterization," In: *Proceedings of the 2018 Manufacturing Science and Engineering Conference - MSEC2018*, 2018, pp.1-4.

[106] J. A. Reinbolt et al., "Are patient-specific joint and inertial parameters necessary for accurate inverse dynamics analyses of gait?," *IEEE Trans Biomed Eng*, vol. 54, no.5, pp.782 , 2007

[107] J. Clément et al., "Soft tissue artifact compensation in knee kinematics by multi-body optimization: Performance of subject-specific knee joint models," *J Biomech*, vol. 48, no.14, pp.3796-3802, 2015.

[108] A. El Habachi et al., "Global sensitivity analysis of the joint kinematics during gait to the parameters of a lower limb multi-body model," *Med Biol Eng Comput*, vol. 53, no.7, pp.655-667, 2015.

[109] P. Walker et al., "The effects of knee brace hinge design and placement on joint mechanics," *J Biomech*, vol. 21, no.11, pp.969-974, 1988.

[110] A. Rajagopal et al., "Full-Body Musculoskeletal Model for Muscle-Driven Simulation of Human Gait.," *IEEE Trans. Biomed. Eng*, vol. 63, no.10, pp.2068-2079, 2016.

[111] M. Conconi et al., "Subject-specific model of knee natural motion: a non-invasive approach," In: *Advances in Robot Kinematics 2016*, 2018, pp.255-264.

[112] M. Conconi et al., "A procedure for the definition of a patient-specific kinematic model of the knee joint: an in-vivo validation," In: *X Giornata di Studio Ettore Funaioli*, 2016, pp 215-220.

[113] S. Martelli et al., "Sensitivity of musculoskeletal models to planar simplification of tibiofemoral motion," In: *8th World Congress of Biomechanics - WCB 2018*, 2018, paper O1495.

[114] G. T. Yamaguchi and F. E. Zajac, "A planar model of the knee joint to characterize the knee extensor mechanism," *J Biomech*, vol. 22, no.1, pp.1-10, 1989.

[115] V. Richard et al., "Comparative assessment of knee joint models used in multi-body kinematics optimisation for soft tissue artefact compensation," *J Biomech*, vol. 62, pp.95-101, 2017

[116] N. Sancisi et al., "A multi-body optimization framework with a knee kinematic model including articular contacts and ligaments," *Meccanica*, vol. 52, no.3, pp.695-711, 2017.

[117] K. Smale et al., "Effect of implementing magnetic resonance imaging for patient-specific OpenSim models on lower-body kinematics and knee ligament lengths," *J Biomech*, in Press.

[118] K. Smale et al., et al, "Relationship of Knee Forces to Subjective Function Pre and Post ACL Reconstruction", *Med. Sci. Sports Exerc.*, 2019.

[119] T. G. Tienen et al., "Displacement of the medial meniscus within the passive motion characteristics of the human knee joint: an RSA study in human cadaver knees," *Knee Surg Sports Traumatol Arthrosc*, vol. 13, no.4, pp.287-292, 2005.

[120] M. Conconi and V. Parenti-Castelli, "Functional Modeling of Human Joints: A Feasibility Study for the Knee," In: *Proceedings of IDETC/CIE Conference*, 2013, pp..V004T08A007.